

# THE EFFECT OF HIGH ENERGY MILLING ON THE MICROSTRUCTURE AND MECHANICAL PROPERTIES OF A Ti-13Nb-13Zr ALLOY PRODUCED BY POWDER METALLURGY

J. H. Duvaizem<sup>1</sup>, S. C. Silva<sup>1</sup>, A. H. Bressiani<sup>1</sup>, R. N. de Faria<sup>1</sup>, H. Takiishi<sup>1</sup>  
Av. Lineu Prestes, 2242, 05508-000 - São Paulo - SP - jduvaizem@ipen.br

<sup>1</sup> Instituto de Pesquisas Energéticas e Nucleares

## ABSTRACT

*In this work the effects of the milling stage upon the microstructures and mechanical properties of a Ti-13Nb-13Zr alloy produced by powder metallurgy have been studied. Powder alloys have been produced via high energy planetary ball milling and also using conventional ball milling for a comparison. Samples were isostatically pressed at 200 MPa and sintered at 1150 °C for 7, 10 and 13 hours. Elastic modulus and microhardness were determined using a dynamic mechanical analyzer and a Vickers microhardness tester. Microstructures and phases were observed and analyzed employing scanning electron microscopy and X-ray diffraction. A Ti-13Nb-13Zr alloy with good biomechanical characteristics has been produced by sintering the hydride milled materials at 1150 °C for 10 hours.*

Key-words: Titanium Alloys, Ti-13Nb-13Zr alloy, Biomaterials, Hydrogenation.

## INTRODUCTION

Hydrogen has been used as a pulverizing agent for rare earth-transition metals alloys due to its extremely high diffusion rate at low and high temperatures<sup>(1)</sup>. Biocompatible alloys are being studied with great emphasis on corrosion behavior, surface properties and biocompatibility on implants<sup>(2)</sup>. Titanium and its alloys show lower elastic modulus, superior biocompatibility and enhanced corrosion resistance<sup>(3,4)</sup>. However, the use of titanium alloys has been limited to commercially pure titanium (Ti<sub>Cp</sub>) and Ti-6Al-4V alloy<sup>(4)</sup>. Notwithstanding, in recent years vanadium has been found to

cause cytotoxic effects and adverse tissue reactions and aluminum has been associated with potential neurological disorders<sup>(5-9)</sup>. Recently, Ti-13Nb-13Zr alloy has been developed and classified as totally biocompatible. This alloy shows low modulus of elasticity and high mechanical properties<sup>(10)</sup>. The advantage of obtaining titanium alloys by powder metallurgy is to produce a porous structured shape which is a requirement for application in dental implants<sup>(11)</sup>. Other advantages include better surface finishing, better homogeneity and near-net-shape of the final product<sup>(10)</sup>. In this study, hydrogen has been used to pulverize Ti, Nb and Zr to produce, by powder metallurgy, a Ti-13Nb-13Zr alloy. Microstructures and physical properties have also been studied.

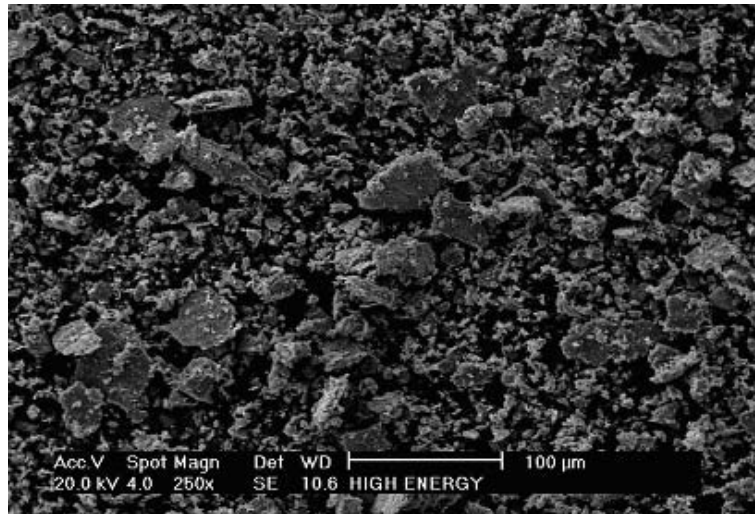
## EXPERIMENTAL

Titanium, niobium and zirconium were heat treated under a hydrogen atmosphere at temperatures of 700, 600 and 500 °C, respectively, and then mechanically broken in small particles (<425 µm). The hydride powder was weighted, Ti - 74%, Nb - 13%, Zr - 13% (%wt) and milled in high energy planetary ball milling (HEPBM) at 200 rpm for 90 minutes and also, for a comparison, in a conventional ball milling (CBM) for 30 hours. The milled powders were isostatically pressed at 200 MPa and sinterized on the temperature of 1150 °C for 7, 10 and 13 hours under high vacuum.

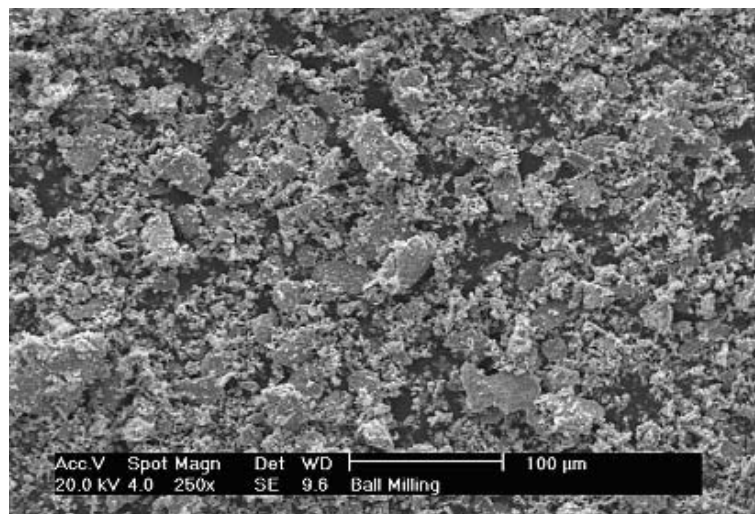
Microstructures and phases were characterized using scanning electron microscopy (SEM) and X-ray diffraction (XRD). Density and porosity were determined via Archimedes method using water as liquid displacement, microhardness using a Vickers microhardness tester and elastic modulus using a dynamic mechanical analyzer (DMA). Particle size distribution was determined utilizing CILAS 1064 equipment.

## RESULTS AND DISCUSSION

Figures 1a and b show SEM microstructures of the Ti-13Nb-13Zr hydride powders milled using high energy planetary ball milling and conventional ball milling, respectively. The structures of these powders are somewhat distinct. The former shows a more homogeneous particle structure.



(a)



(b)

Figure 1 – SEM microstructure of the Ti-13Nb-13Zr hydride milled powders: (a) HEPBM 200 rpm for 90 min and (b) CBM for 30 h.

Figure 2 shows the particle size distribution of these materials obtained via CILAS. CBM yielded a larger particle size distribution than HEPBM. The higher concentration of thin particles was attributed to the milling time. Although average particle size is larger in the HEPBM powder, the distribution size is more uniform than that of the CBM powder. Larger plates were identified as Ti and Nb, showing that the hydrogenation process was less effective for these elements.

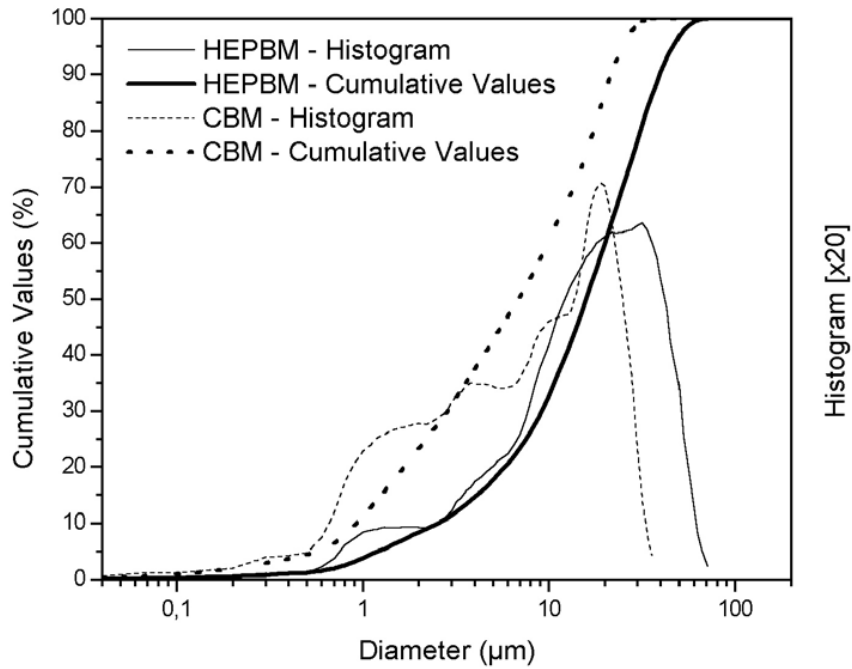
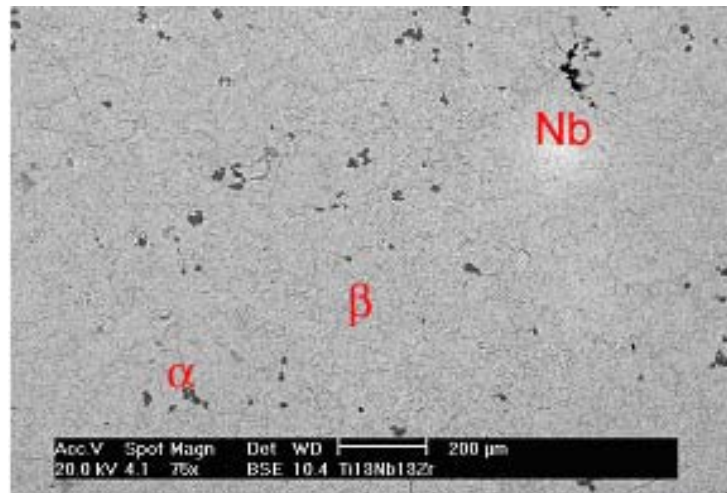
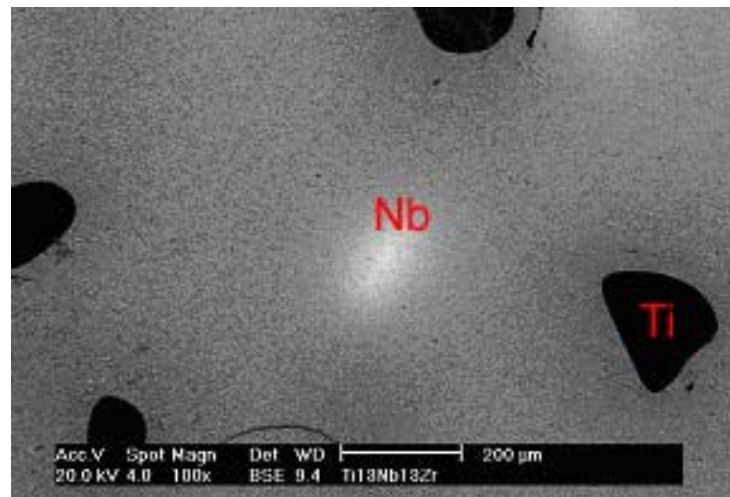


Figure 2 – Particle size distribution obtained for the Ti-13Nb-13Zr hydride milled powder via CILAS (HEPBM and CBM).

Figures 3a and b show the microstructure of the Ti-alloy sintered at 1150 °C and milled for 7 h. Some areas containing unreacted materials can be seen. The HEPBM sample shows only a small area containing Nb and formation of a  $\alpha+\beta$  phase. Conversely, the CBM sample exhibited large areas containing free Ti and Nb. This can be attributed to the major concentration of thin particles which difficult the interaction with Ti.



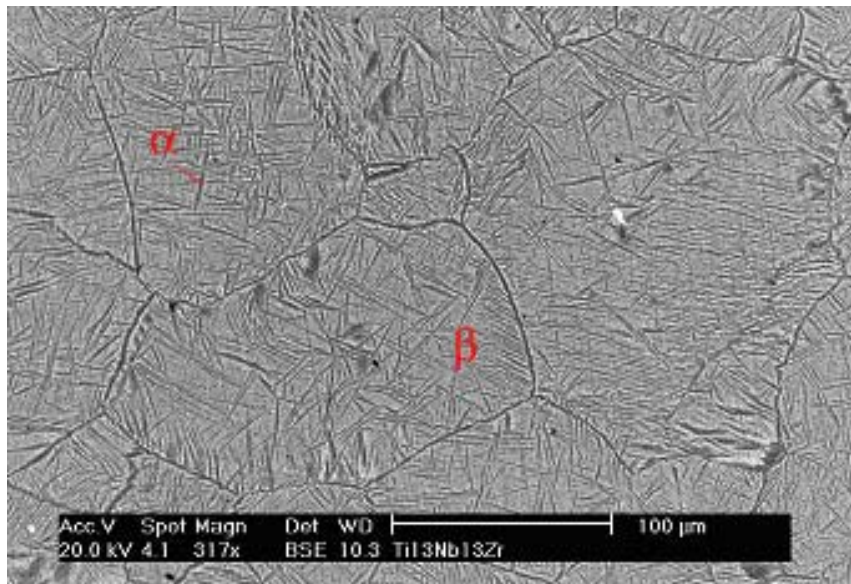
(a)



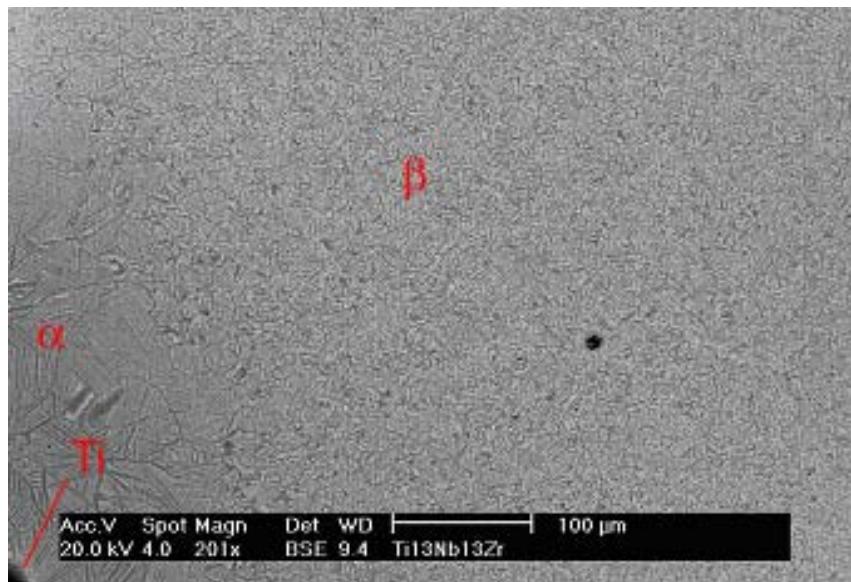
(b)

Figure 3 – Ti-13Nb-13Zr material produced with powder obtained via HEPBM (a) and CBM (b) and sintered at 1150°C for 7 h.

Figures 4a and b shows the microstructures of HEPBM and CBM samples sintered for 7 h. In the former,  $\alpha$  and  $\beta$  phases are present whereas in the material produced via CBM they are present only on the free titanium boundaries. The large amount of thin particle yielded a non-homogeneous grains size (and phases) in the CBM sample.



(a)

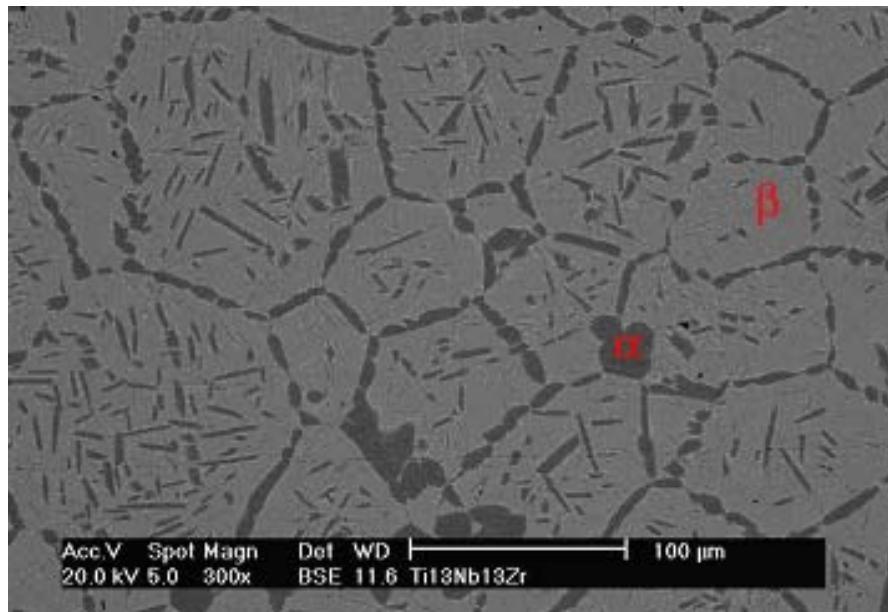


(b)

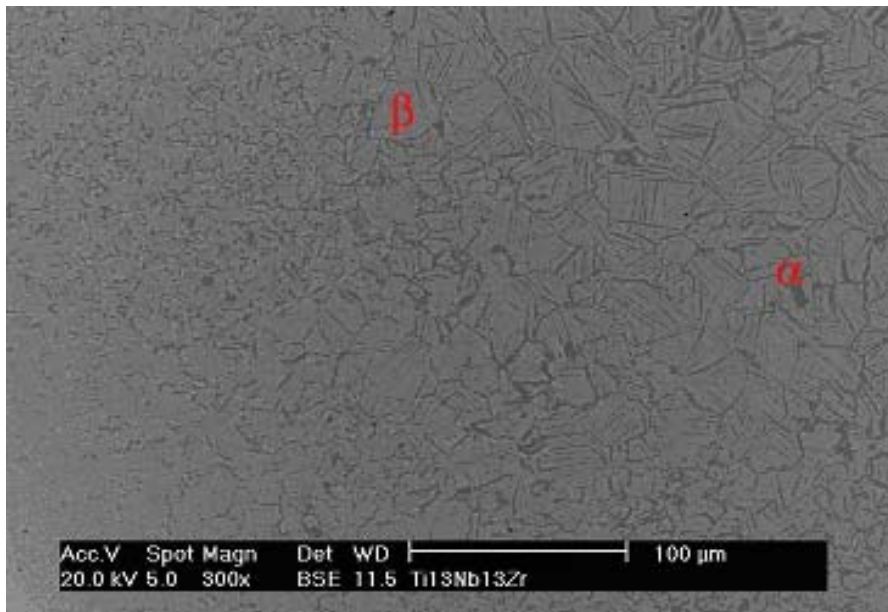
Figure 4 – Backscattered electron images of the Ti-13Nb-13Zr material sintered at 1150°C for 7 h and produced with powder obtained via HEPBM (a) and CBM (b).

Figures 5a and b shows the microstructures of the samples produced with HEPBM and CBM, sintered for 10 h, respectively. In this condition, areas containing free niobium are no longer observed in the HEPBM sample. Conversely, the sample produced with

CBM still shows large areas containing free titanium and niobium and it is not homogeneous.



(a)



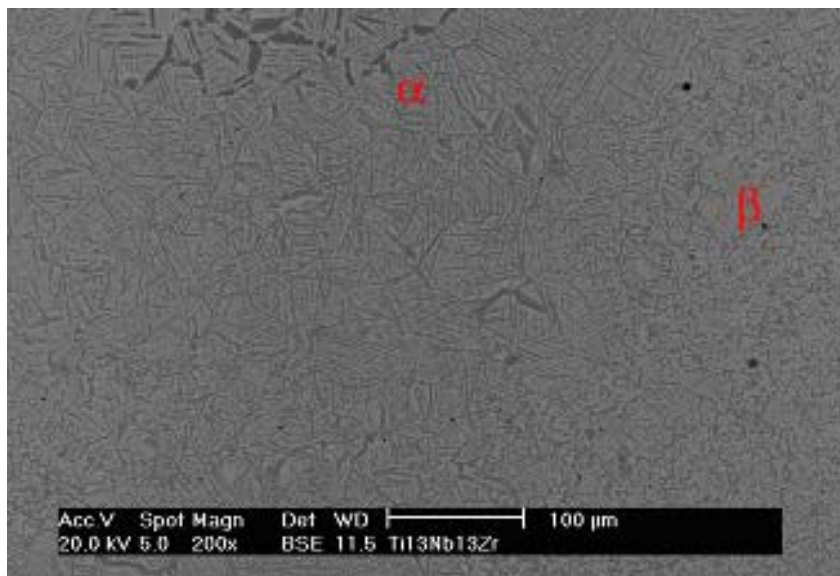
(b)

Figure 5 – Backscattered electron images of the Ti-13Nb-13Zr material sintered at 1150°C for 10 h and produced with powder obtained via HEPBM (a) and CBM (b).

Figure 6a and b shows the microstructures of HEPBM and CBM samples sintered for 13 h, respectively. The latter still shows large areas with free Ti and Nb while the former only presents  $\alpha$  and  $\beta$  phases, showing the superior performance of the HEPBM process.



(a)



(b)

Figure 6 – Backscattered electron images of the Ti-13Nb-13Zr material sintered at 1150°C for 13 h and produced with powder obtained via HEPBM (a) and CBM (b).



Density, porosity, microhardness and elastic modulus of samples produced via HEPBM and CBM are given in Table 1. A superior densification for the samples produced via HEPBM can be readily noted. The microhardness and elastic modulus are also superior for the samples produced via HEPBM. The microhardness values for the sample produced via CBM show a decrease and then an increase for the sintering times of 10 and 13 hours, respectively. This can be attributed to the non homogeneous microstructure. The elastic modulus increases rapidly with increasing sintering time for the HEPBM alloys. This is observed only for the CBM alloy sintered for 13 h.

**Table 1** – Density, porosity, microhardness and elastic modulus values obtained for the Ti-13Nb-13Zr alloys.

| Sample identification | Density (g/cm <sup>3</sup> )<br>(±0.02) | Porosity (%)<br>(±0.2) | Microhardness (HV) | Elastic Modulus (GPa) |
|-----------------------|---|------------------------|--------------------|-----------------------|
| HEPBM - 7h            | 4.94                                    | 1.3                    | 437 ± 25           | 81.3                  |
| HEPBM -10h            | 4.98                                    | 1.0                    | 459 ± 25           | 88.2                  |
| HEPBM - 13h           | 5.00                                    | 0.5                    | 465 ± 25           | 89.5                  |
| CBM - 7h              | 4.64                                    | 4.9                    | 385 ± 40           | 76.4                  |
| CBM - 10h             | 4.70                                    | 1.3                    | 320 ± 40           | 76.3                  |
| CBM - 13h             | 4.71                                    | 1.9                    | 346 ± 40           | 78.0                  |

Figures 7 and 8 show the XRD patterns of the samples produced via HEPBM and CBM, respectively. Although MEV analysis shows that the CBM sample contain free niobium, only  $\alpha$  and  $\beta$  phase of Ti were identified by X-ray diffraction.

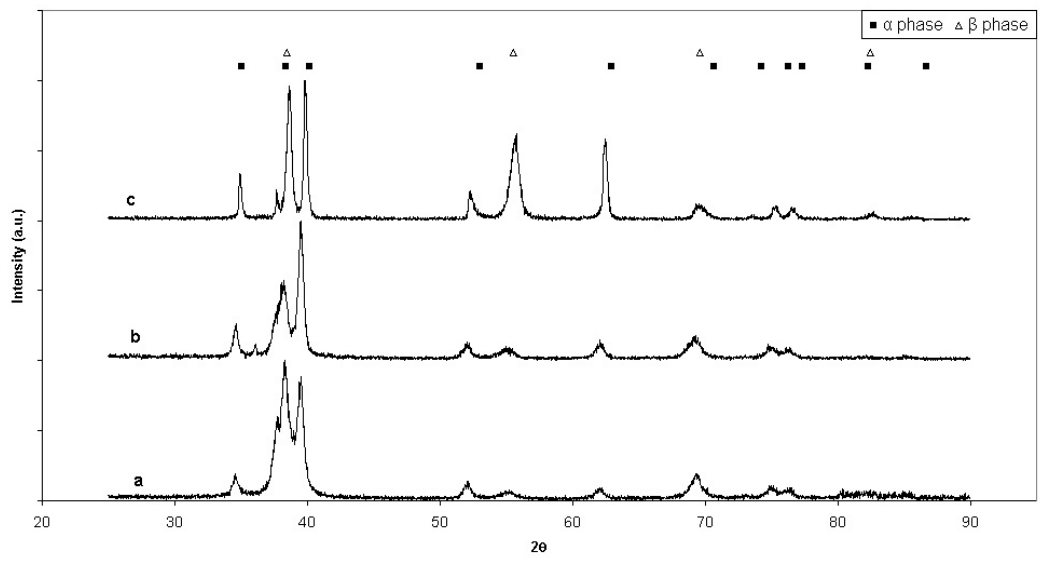


Figure 7 – XRD patterns of the Ti-13Nb-13Zr alloy produced via HEPBM and sintered for (a) 7, (b) 10 and (c) 13 h.

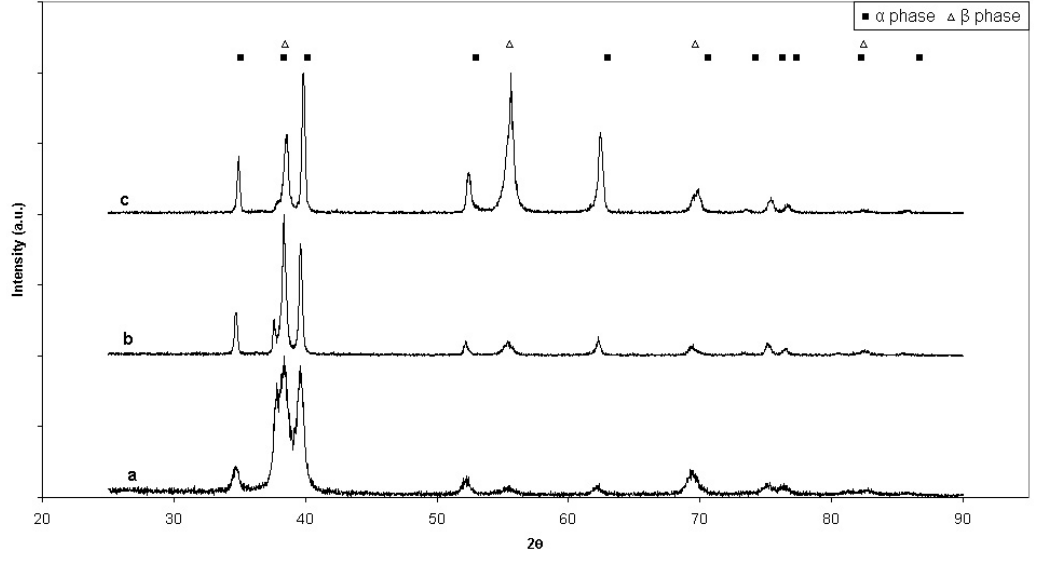


Figure 7 – XRD patterns of the Ti-13Nb-13Zr alloy produced via CBM and sintered for (a) 7, (b) 10 and (c) 13 h.

## CONCLUSION

It has been shown that high energy planetary ball milling is more efficient than conventional ball milling to produce a Ti-13Nb-13Zr alloy. The former yielded a more uniform particle size distribution. Alloys produced via high energy planetary ball milling also showed superior microstructural homogeneity than those produced via conventional ball milling, although with higher microhardness and elastic modulus. It is feasible to produce a Ti-13Nb-13Zr alloy by powder metallurgy using a sintering temperature of 1150 °C.

## ACKNOWLEDGMENTS

Many thanks are due to FAPESP, CNPQ and IPEN-CNEN/SP for supporting this investigation. Thanks are due to L. F. C. P. Lima for the DMA analyses.

## REFERENCES

1. India. Department of Atomic Energy, Hydrogen in metals, ***Proceedings of the Interdisciplinary Meeting on Hydrogen in Metals***, Bombay, February 19-20, 1980.
2. OLIVEIRA, N. T. C. ; BIAGGIO, S. R. ; NASCENTE, P. A. P. ; ROCHA-FILHO, R. C. ; BOCCHI, N., Investigation of passive films grown on biocompatible Ti-50Zr and Ti-13Nb-13Zr alloys by XPS. ***Surface and Interface Analysis***, v.38, n. 4, p. 410-412, 2006.
3. DAVIDSON, J. A. ; MISHRA, A. K. ; KOVACS, P. ; POGGIE, R. A., ***Bio-Medical Materials Engineering*** 4, p. 231 – 243, 1994.
4. EISENBARTH, E.; VELTEN, D.; MULLER, M.; THULL, R.; BREME, J. Biocompatibility of beta-stabilizing elements of titanium alloys. ***Biomaterials***, v.25, n. 26, p. 5705-5713, 2004.
5. GEETHA, M. ; SINGH. A. K. ; MURALEEDHARAN, K. ; GOGIA, A. K. ; ASOKAMANI, R., Effect of thermochemical processing on microstructure of a Ti-13Nb-13Zr alloy, ***Journal of Alloys and Compounds***, v.329, p. 264 – 271, 2001.
6. S.G. Steinemann, in: ***Evaluation of Biomaterials***, Wiley, New York, 1980, p. 1–34.
7. P.G. Laing, A.B. Ferguson Jr, E.S. Hodge, ***Journal of Biomedical Materials Research*** 1(1967) 135–149.

8. D.R.C. McLachlan, B. Farnell, H. Galin, in: B. Sarkar (Ed.), ***Biological Aspects of Metals and Metal - Related Diseases***, Raven Press, New York, 1983, p. 209–218.
9. D.P. Perl, A.R. Brody, *Science* 208 (1980) 297–299.
10. HENRIQUES, V.A.R.; SILVA, C.R.M.; BRESSIANI, J.C. Utilização de Técnicas de Metalurgia do Pó (M/P) na Obtenção da Liga Ti-13Nb-13Zr, ***Revista Metalurgia e Materiais***, v.59, nº 532, abril 2003.
11. KUTTY, M.G.; BHADURI, S.; BHADURI, S.B. Gradient surface porosity in titanium dental implants: relation between processing parameters and microstructure. ***Journal of Materials Science - Materials in Medicine***, v.15, p. 145-150, 2004.